Published Ahead of Print on June 8, 2016 as 10.5966/sctm.2015-0263.

STEM CELLS TRANSLATIONAL MEDICINE®

TISSUE ENGINEERING AND REGENERATIVE MEDICINE

Bone Marrow Mesenchymal Stem Cell-Based Engineered Cartilage Ameliorates Polyglycolic Acid/Polylactic Acid Scaffold-Induced Inflammation Through M2 Polarization of Macrophages in a Pig Model

JINPING DING, BO CHEN, TAO LV, XIA LIU, XIN FU, QIAN WANG, LI YAN, NING KANG, YILIN CAO, RAN XIAO

Key Words. Cartilage tissue engineering • Bone marrow mesenchymal stem cells • Scaffold-induced inflammation • Macrophage polarization • Immunocompetent

Research Center of Plastic Surgery Hospital, Chinese Academy of Medical Sciences and Peking Union Medical College, Beijing, People's Republic of China

Correspondence: Ning Kang, M.D., Ph.D., Research Center of Plastic Surgery Hospital, Chinese Academy of Medical Sciences & Peking Union Medical College, No. 33 Ba-Da-Chu Road, Shi Jing Shan District, Beijing 100144, People's Republic of China. Telephone: 86 10 88771507; E-Mail: ningkang1983@yahoo.com; or Yilin Cao, M.D., Ph.D., Research Center of Plastic Surgery Hospital, Chinese Academy of Medical Sciences & Peking Union Medical College, No. 33 Ba-Da-Chu Road, Shi Jing Shan District, Beijing 100144, People's Republic of China. Telephone: 86 10 88771507; E-Mail: yilincao@yahoo.com; or Ran Xiao, D.D.S., M.D., Research Center of Plastic Surgery Hospital, Chinese Academy of Medical Sciences & Peking Union Medical College, No. 33 Ba-Da-Chu Road, Shi Jing Shan District, Beijing 100144, People's Republic of China. Telephone: 86 10 88771507; E-Mail: xiaoran@pumc.edu.cn

Received September 26, 2015; accepted for publication March 14, 2016.

1066-5099/2016/$20.00/0

http://dx.doi.org/10.5966/sctm.2015-0263

ABSTRACT

The regeneration of tissue-engineered cartilage in an immunocompetent environment usually fails due to severe inflammation induced by the scaffold and their degradation products. In the present study, we compared the tissue remodeling and the inflammatory responses of engineered cartilage constructed with bone marrow mesenchymal stem cells (BMSCs), chondrocytes, or both and scaffold group in pigs. The cartilage-forming capacity of the constructs in vitro and in vivo was evaluated by histological, biochemical, and biomechanical analyses, and the inflammatory response was investigated by quantitative analysis of foreign body giant cells and macrophages. Our data revealed that BMSC-based engineered cartilage suppressed in vivo inflammation through the alteration of macrophage phenotype, resulting in better tissue survival compared with those regenerated with chondrocytes alone or in combination with BMSCs. To further confirm the macrophage phenotype, an in vitro coculture system established by engineered cartilage and macrophages was studied using immunofluorescence, enzyme-linked immunosorbent assay, and gene expression analysis. The results demonstrated that BMSC-based engineered cartilage promoted M2 polarization of macrophages with anti-inflammatory phenotypes including the upregulation of CD206, increased IL-10 synthesis, decreased IL-1β secretion, and alterations in gene expression indicative of M1 to M2 transition. It was suggested that BMSC-seeded constructs have the potential to ameliorate scaffold-induced inflammation and improve cartilaginous tissue regeneration through M2 polarization of macrophages. STEM CELLS TRANSLATIONAL MEDICINE *2016;5:1–11*

SIGNIFICANCE

Finding a strategy that can prevent scaffold-induced inflammation is of utmost importance for the regeneration of tissue-engineered cartilage in an immunocompetent environment. This study demonstrated that bone marrow mesenchymal stem cell (BMSC)-based engineered cartilage could suppress inflammation by increasing M2 polarization of macrophages, resulting in better tissue survival in a pig model. Additionally, the effect of BMSC-based cartilage on the phenotype conversion of macrophages was further studied through an in vitro coculture system. This study could provide further support for the regeneration of cartilage engineering in immunocompetent animal models and provide new insight into the interaction of tissue-engineered cartilage and macrophages.

INTRODUCTION

Cartilage tissue engineering has made great progress in recent years. The repair of articular defects by using engineered cartilage has been extensively investigated in animal models and clinical trials [1, 2]. However, cartilage regeneration at ectopic sites usually fails in immunocompetent animals, owing to severe subcutaneous inflammation caused by the engineered implants [3, 4]. Some literature showed that the subcutaneous autotransplantation of engineered cartilage in canine, swine, or rabbit models finally resulted in complete absorption, accompanied by strong inflammatory responses [3, 5]. In other advanced cases, subcutaneous harvesting of the remnants of the engineered cartilage from immunocompetent animals found them to be structurally immature and nonuniform, with fibrous and vascular tissue invasion accompanied by many inflammatory cells. Therefore, a major challenge in achieving effective ectopic cartilage regeneration in the immunocompetent environment is the

Published Ahead of Print on June 8, 2016 as 10.5966/sctm.2015-0263.

prevention of inflammatory reactions, which is the main factor limiting cartilage tissue engineering in clinical application.

Recent studies have indicated that the inflammatory response is primarily induced by biomaterials and/or their degradation products, regardless of whether they are biologically or artificially synthesized scaffolds [3, 4, 6]. Although collagen-based cartilage was successfully engineered in the subcutaneous environment of an ovine model [7], it was suggested that the collagen was not adapted to engineering cartilage with specific shape and firmness because of its fast degradation. Polymer scaffolds, exhibiting predictable and reproducible mechanical and physical properties such as elastic modulus and degradation rate [8, 9], have drawn great attention in cartilage engineering. However, construction of a polymer scaffold-based cartilage with good inflammatory control still remains a challenge. Another study found that stimulation of Fas ligand overexpressing on chondrocytes could induce host macrophage apoptosis and further improve the survival of poly(L-lactic acid)-based engineered cartilage in a mouse model [10], the results of which have yet to be reproduced in large animals. Zheng et al. used a closed chamber to separate implants from the invasion of host cells and vasculature to partially inhibit the inflammatory reaction [11], but this technique reduced nutrient exchange and negatively affected tissue development.

Owing to their immunoprivileged and immunomodulatory capacities, bone marrow mesenchymal stem cells (BMSCs) have shown good potential for therapeutic application in inflammatory diseases, such as lung fibrosis, lung sepsis, and peritonitis [12–18]. BMSCs are also widely investigated in cartilage tissue engineering because of their remarkable potential for proliferation and chondrogenesis [19–22]. BMSC-based engineered cartilage showed similarities in tissue structure and the biochemical and biomechanical properties compared with cartilage regenerated with chondrocytes. Within and around biomaterial implants, transient neutrophil accumulation followed by sustained and robust infiltration of macrophages is a common inflammatory process. Interactions between BMSCs and macrophages have been demonstrated to play an important role in the inflammation control and induction of tissue remodeling. For example, a poly(ethylene glycol) hydrogel encapsulated with BMSCs reduced tumor necrosis factor-α (TNF-α) release by attenuating the infiltration of M1 macrophages, leading to a weak foreign body reaction manifested by a thinner fibrous capsule and improved tissue survival in the long-term [23]. Geng et al. suggested that rhabdomyolysis-induced acute kidney injury (AKI) in mice infused with M0 and M1 macrophages suffered more severe renal functional impairment, whereas injection of MSCs can ameliorate AKI through the activation of macrophages to a trophic M2 phenotype characterized by an increased expression of CD206 and interleukin-10 [24]. These results indicate that MSCs exhibit great potential for anti-inflammation through macrophage modulation.

With these promising findings, questions are raised as to whether BMSC-based engineered cartilage could ameliorate polymer scaffold-induced inflammation through macrophage modulation. In the present study, we examined the use of BMSCs, or auricular chondrocytes, alone or in combination with each other, constructed with a polyglycolic acid (PGA)/polylactic acid (PLA) scaffold, to induce the formation of tissue-engineered cartilage subcutaneously in a pig model. The cartilage-forming capacity in vitro and in vivo of each group was systematically evaluated by histological, biochemical, and biomechanical examinations, and the inflammatory responses were investigated by quantitative analysis of foreign body multinucleated giant cells (FBGCs) and macrophage phenotype. Moreover, an in vitro coculture system was established to further confirm the interaction between engineered cartilage and macrophages. This study could provide further support for cartilage engineering in immunocompetent animal models and bring new insight into the interaction of tissue-engineered cartilage and macrophages.

Materials and Methods

Cell Culture

Animal experiments were approved by the Ethics Committee of Peking Union Medical College. Bone marrow and auricular cartilage were obtained from iliac crests and external ears, respectively, of 50-day-old pigs (n = 3). As previously described [25], BMSCs were isolated and cultured in low-glucose (1,000 mg/l) Dulbecco's modified Eagle's medium (L-DMEM, GE Healthcare Life Sciences, Piscataway, NJ, http://www.gelifesciences.com) supplemented with 10% fetal bovine serum (FBS, Thermo Fisher Scientific Life Sciences, Waltham, MA, http://www.thermofisher.com), 100 U/ml penicillin, and 0.1 mg/ml streptomycin at 37°C with 95% humidity and 5% CO_2. Part of the auricular cartilage specimen was used for biomechanical and biochemical evaluations, and the rest was fragmented into 1-mm^3 pieces and digested with 0.25% trypsin for 30 minutes, followed by 0.2% type IV collagenase (Sigma-Aldrich, St. Louis, MO, http://www.sigmaaldrich.com) for 8 hours at 37°C on a shaker. The isolated cells were cultured and subcultured at a density of 2.5×10^4 cells per cm^2 in high-glucose Dulbecco's modified Eagle's medium (H-DMEM; 4,500 mg/l) supplemented with 10% FBS, 100 U/ml penicillin, and 0.1 mg/ml streptomycin. Passage 2 BMSCs and chondrocytes were harvested for cartilage construction. The porcine alveolar macrophage (PAM) cell line 3D4/21 (CRL-2843), established by transformation of PAMs with SV40 large T antigen, was purchased from the American Type Culture Collection (Manassas, VA, http://www.atcc.org) and maintained in RPMI 1640 medium, supplemented with 10% FBS, at a density of 1.7×10^5 cells per cm^2 [23].

Fabrication of PGA/PLA Scaffolds

Unwoven PGA fibers (provided by National Tissue Engineering Research Center, Shanghai, People's Republic of China, http://en.sjtu.edu.cn/research/centers-labs/national-tissue-engineering-research-center) were pressed into a cylinder shape of 13-mm diameter and 1.5-mm thickness. A solution of 0.5% PLA (wt/vol; Sigma-Aldrich) diluted in dichloromethane was dropped evenly onto the PGA mesh to solidify each scaffold [25, 26]. The PGA/PLA scaffold exhibited appropriate pore structures with the cross-linked fibers (supplemental online Fig. 1). The scaffolds (n = 96) were soaked in 75% alcohol for 12 hours and washed three times with phosphate-buffered saline (PBS), followed by DMEM containing 10% FBS preculturing overnight.

Group Design and In Vitro Cartilage Construction

Three groups of cell-scaffold complexes (n = 24 per group) were constructed as follows: BMSCs (P2), auricular chondrocytes (ACs) (P2), or an equal combination of both (1:1) were seeded at a

Published Ahead of Print on June 8, 2016 as 10.5966/sctm.2015-0263.

Table 1. Primer sequences used for real-time polymerase chain reaction

Gene	Forward primer	Reverse primer
GAPDH	5-CTGCCCCTTCTGCTGATGC-3	5-TCCACGATGCCGAAGTTGTC-3
IL-1β	5-TTCTCCTCACTCAAAGCCAG-3	5-CACACTCACCCCAAAGAAAT-3
TNF-α	5-CGCATCGCCGTCTCCTACCA-3	5-GCCCAGATTCAGCAAAGTCCAGAT-3
IL-6	5-CTGGCAGAAAACAACCTGAACC-3	5-TGATTCTCATCAAGCAGGTCTCC-3
NOS2	5-CTCCAGGTGCCCACGGGAAA-3	5-TGGGGATACACTCGCCCGCC-3
IL-10	5-GGATGACGACTCTACTAAAC-3	5-TTGAACACCATAGGGCACAC-3
TGF-β	5-CACGTGGAGCTATACCAGAA-3	5-TCCGGTGACATCAAAGGACA-3
Arg-1	5-AGAAGAACGGAAGGACCAGC-3	5-CAGATAGGCAGGGAGTCAC-3
CXCR2	5-TGCCTCAATCCTCTCATCTAC-3	5-TGGCTCAGAATGGACACCGA-3
CCR1	5-GTGCTGCCTCTATTGGTCAT-3	5-ACCTCTGTCACTTGTATGGC-3
CCR2	5-CTCCCTCTCTGATTCTACCT-3	5-ACAGTTCTCAAGCTCTCCAT-3
CCR4	5-TTCAAGTACAAGCGGCTCAAG-3	5-CAGGTACCTATCGATGCTCAT-3
CX3CR1	5-TTTGCGAATGTCAGGGAGG-3	5-GCGAAGAAAGCCAGGATGAG-3

Abbreviations: *Arg-1*, Arginase 1; *CCR1*, chemokine (C-C motif) receptor type 1; *CCR2*, chemokine (C-C motif) receptor type 2; *CCR4*, chemokine (C-C motif) receptor type 4; *CXCR2*, chemokine (C-X-C motif) receptor type 2; *CX3CR1*, chemokine (C-X3-C motif) receptor type 1; *GAPDH*, glyceraldehyde-3-phosphate dehydrogenase; *IL-1β*, interleukin-1β; *IL-6*, interleukin 6; *IL-10*, interleukin 10; *NOS2*, nitric oxide synthase 2; *TGF-β*, transforming growth factor β; *TNF-α*, tumor necrosis factor α.

density of 6×10^7 cells per milliliter onto each PGA/PLA scaffold, followed by 5-hour incubation to promote cell adhesion [25, 26]. PGA/PLA scaffolds without cells were used as a control. All the samples were statically cultured in FBS-free H-DMEM, supplemented with 10 ng/ml transforming growth factor β3 (TGF-β3; Peprotech, Rocky Hill, NJ, http://www.peprotech.com), 100 ng/ml insulin-like growth factor (R&D Systems Inc., Minneapolis, MN, https://www.rndsystems.com), 40 ng/ml of dexamethasone (Sigma-Aldrich), 0.2 mM of ascorbic acid, and ×1 insulin-transferrin-selenium (Sigma-Aldrich) for 8 weeks in vitro. Medium was refreshed every 2 days.

Subcutaneous Implantation

After 8 weeks, constructs from BMSC, AC, 1:1, or PGA/PLA scaffold control groups ($n = 12$ per group) were autotransplanted into individual subcutaneous pockets and harvested after 2, 4, and 8 weeks of implantation for analyses.

Histological and Immunohistochemical Examinations

Samples from each group were harvested after 8 weeks in vitro and 72 hours and 2, 4, and 8 weeks in vivo, and subjected to histological and immunohistochemical examinations. The specimens were fixed with 10% buffered formalin in PBS for 48 hours, embedded in paraffin, sectioned into 5-mm sections, and then stained with hematoxylin and eosin (H&E) and Safranin O. Type II collagen expression was detected by using a mouse anti-human type II collagen monoclonal antibody (1:100; Zhongshanjinqiao, Beijing, People's Republic of China, http://www.zsbio.com/) followed by horseradish peroxidase-conjugated anti-mouse antibody and color development with diaminobenzidine tetrahydrochloride (Zhongshanjinqiao).

Quantification of Glycosaminoglycan, Total Collagen, and Young's Modulus

After 8 weeks of in vitro culture, glycosaminoglycan (GAG) content was analyzed by using spectrophotometric microdetermination by the dimethylmethylene blue chloride (Kamiya Biomedical, Seattle, WA, http://www.kamiyabiomedical.com) method, and total collagen content was quantified by hydroxyproline assay as previously described [26]. To examine the mechanical properties, samples were tested by using a biomechanical analyzer (Instron, Canton, MA, http://www.instron.us), and the superficial area and thickness were measured ($n = 3$ per group). Porcine auricular cartilage was used as a positive control ($n = 3$). A constant compressive strain rate of 0.3 mm/minute was applied until 80% of maximal deformation was achieved and a stress-strain curve was generated. Young's modulus was calculated based on the formula $Y = S \times T/A$ (Y, Young's modulus; S, slope of stress-strain curve; T, thickness; A, superficial area).

Quantification of Residual PGA/PLA Scaffold

After 8 weeks of in vitro culture, images at ×200 magnification ($n = 6$) from H&E-stained sections were randomly selected, and the percentage of the area containing PGA/PLA was calculated by using image-processing software (Image-Pro Plus, version 3.0, Media Cybernetics, Rockville, MD, http://www.mediacy.com).

Examinations of FBGCs and Macrophages

Images adjacent to the implant obtained at ×400 magnification ($n = 6$) from the H&E-stained sections were randomly acquired, and the total number of FBGCs was counted. By microscopy, FBGCs were defined as large cells containing more than two nuclei.

To characterize the macrophage phenotype, immunofluorescent labeling of primary antibodies against the pan-macrophage marker CD68 (goat anti-mouse CD68, 1: 50, Santa Cruz Biotechnology, Santa Cruz, CA, http://www.scbt.com) and the M2 macrophage marker CD206 (rabbit anti-human CD206, 1:50, Santa Cruz Biotechnology) were performed, followed by the fluorescently conjugated secondary antibodies donkey anti-goat Alexa Fluor 488 (1:200 dilution; Abcam, Cambridge, MA, http://www.abcam.com) and donkey anti-rabbit Alexa Fluor 594 (1:200 dilution; Thermo Fisher Scientific Life Sciences). Nuclei were labeled with 4′,6-diamidino-2-phenylindole (Zhongshanjinqiao).

Published Ahead of Print on June 8, 2016 as 10.5966/sctm.2015-0263.

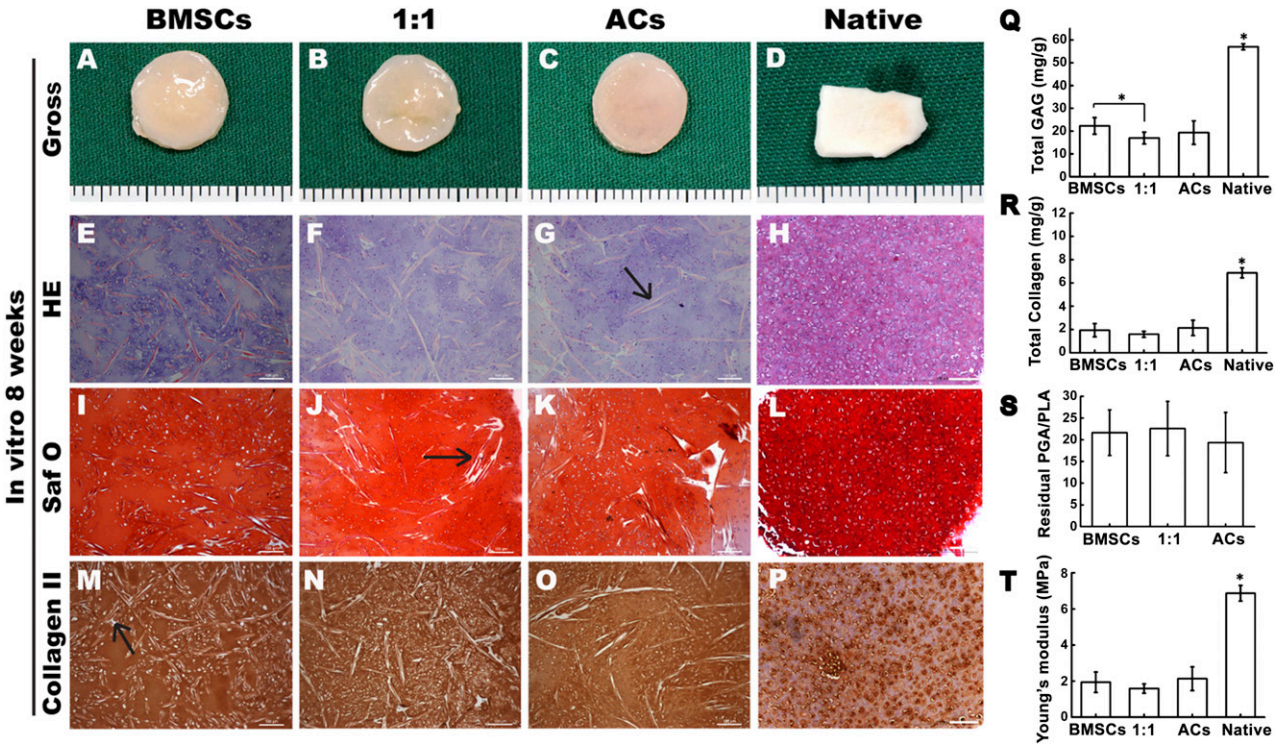

Figure 1. Engineered cartilage construction for 8 weeks in vitro. **(A–C, E–G, I–K, M–O)**: Gross view **(A–C)**, H&E staining **(E–G)**, Safranin O staining **(I–K)**, and immunohistochemical staining of type II collagen **(M–O)**. **(D, H, L, P):** Gross view and histology of pig native auricular cartilage. **(G, J, M):** Black arrows indicate the undegraded PGA fibers. **(Q–T):** Quantitative comparison of the total GAG, total collagen, Young's modulus, and residual PGA/PLA content among the groups of BMSCs, 1:1, and chondrocytes. Scale bars = 100 μm. $*$, $p < .05$ (statistically different from other groups). Abbreviations: ACs, articular chondrocytes; BMSCs, bone marrow mesenchymal stem cells; GAG, glycosaminoglycan; HE, hematoxylin and eosin; PGA, polyglycolic acid; PLA, polylactic acid; Saf O, Safranin O.

Images at $\times$400 magnification ($n = 6$) adjacent to the implant were acquired for quantification of CD68- and CD206-positive macrophages.

In Vitro Coculture of Engineered Cartilage With Macrophages

The macrophage cell line 3D4/21 (CRL-2843), cultured at a density of 2.5×10^5 cells per cm^2, was activated by lipopolysaccharide (LPS; 1 μg/ml) and interferon-γ (IFN-γ; 10 ng/ml) (Peprotech) stimulation for 24 hours before coculture as previously described [10]. In a transwell system with a semipermeable membrane (pore size: 0.4 mm), the engineered cartilage from three groups after 8 weeks in vitro was placed in the upper chamber and cocultured with the activated macrophages seeded in the lower chamber for 24 hours in RPMI 1640 medium supplemented with 10% FBS. The macrophages were subjected to immunofluorescence staining for CD68 and CD206 as described before.

Enzyme-Linked Immunosorbent Assay for Inflammatory Factors

The supernatant of engineered cartilage cocultured with macrophages was collected, and the protein concentrations of interleukin-1β (IL-1β) and interleukin-10 (IL-10) were determined by a commercially available enzyme-linked immunosorbent assay kit (R&D Systems), following the manufacturer's instructions.

Quantitative Real-Time Polymerase Chain Reaction of Inflammation-Related Genes

Macrophages in each coculture group were harvested, and the total RNA was extracted by using TRIzol reagent (Thermo Fisher Scientific Life Sciences). RNA was reverse-transcribed into single-stranded cDNA according to the manufacturer's protocol (Promega, Madison, WI, http://www.promega.com). The expression levels of selected genes were analyzed by quantitative polymerase chain reaction, by using a LightCycler 480 system with a SYBR green kit (Roche Molecular Biochemicals, Mannheim, Germany, http://www.roche.com). The forward and reverse primer pairs are shown in Table 1. To normalize mRNA levels, glyceraldehyde-3-phosphate dehydrogenase was used as an internal housekeeping control.

Scanning Electron Microscopy

The PGA/PLA scaffolds were prepared for scanning electron microscopy examination. Briefly, samples were sputter-coated with gold (BAL-TEC, Philips, Eindhoven, Netherlands, http://www.usa.philips.com) and examined finally with a scanning electron microscope (Philips-XL-30).

Statistical Analysis

Data were presented as mean $\pm$ SD. Statistical significance was evaluated by using one-way analysis of variance in SPSS Statistics 17.0 software. A value of $p < .05$ was considered statistically significant.

Published Ahead of Print on June 8, 2016 as 10.5966/sctm.2015-0263.

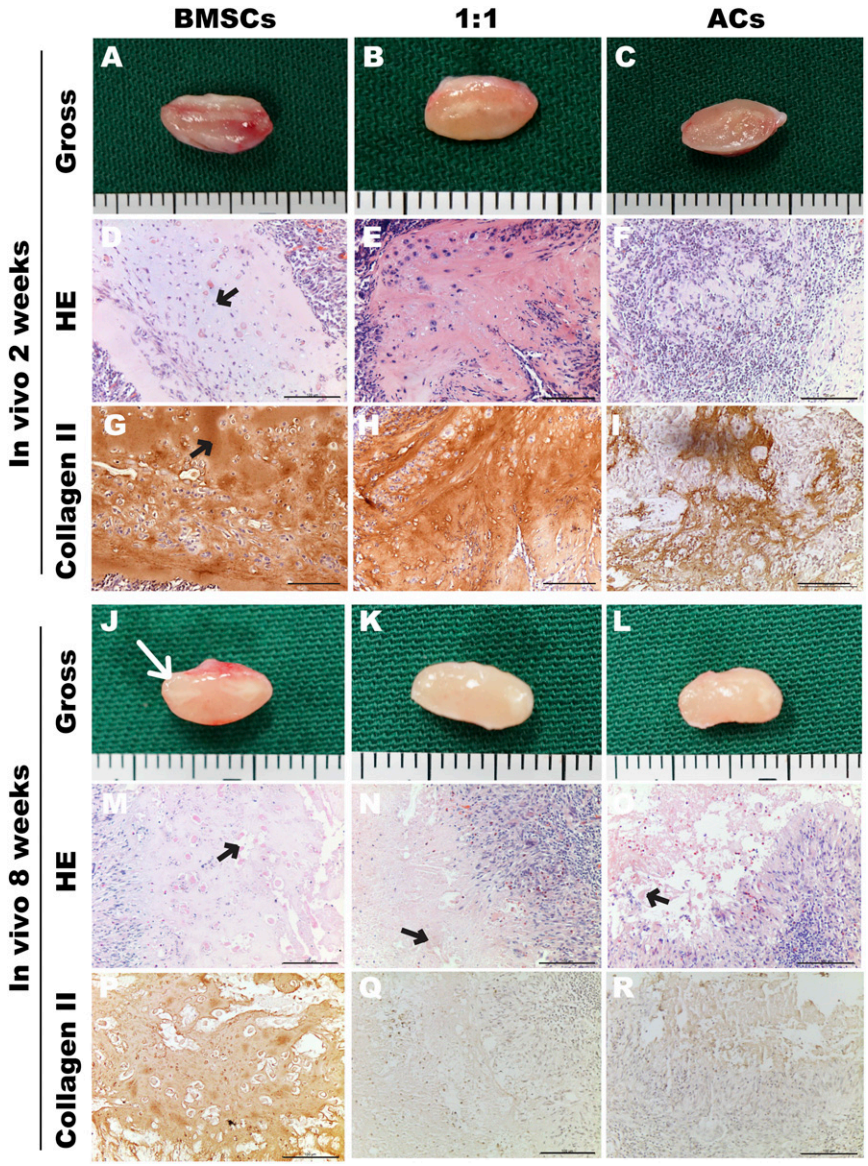

Figure 2. Engineered cartilage construction for 2 and 8 weeks in vivo. Gross view **(A–C, J–L)**, H&E staining **(D–F, M–O)**, and immunohistochemical staining of type II collagen **(G–I, P–R)**. Black arrows indicate homogeneously distributed lacunas **(D)** and intensely deposited type II collagen **(G)** and the undegraded polyglycolic acid fibers **(M–O)**. **(J):** White arrow indicates the outline of the implant. Scale bars = 100 μm. Abbreviations: ACs, articular chondrocytes; BMSCs, bone marrow mesenchymal stem cells; HE, hematoxylin and eosin.

RESULTS

Engineered Cartilage Construction In Vitro

After culturing for 8 weeks in vitro, all cell-scaffold constructs in the BMSC, AC, and 1:1 groups maintained their original round shapes and exhibited an ivory-white-like appearance (Fig. 1A–1C). Samples in all three groups exhibited typical cartilaginous features with lacuna structures (Fig. 1E–1G) and abundant cartilage-specific extracellular matrix deposition, as indicated by positive staining for Safranin O (Fig. 1I–1K) and type II collagen (Fig. 1M–1O). Pig native auricular cartilage was set as control (Fig. 1D, 1H, 1L, 1P). Notably, a few undegraded PGA fibers were observed among the tissues (Fig. 1G, 1J, 1M, indicated by black arrows).

Additionally, quantitative analysis showed that GAG content was significantly higher in the BMSC group than in the 1:1 group ($p < .05$) (Fig. 1Q). Furthermore, no significant differences were found among the three groups in total collagen, Young's modulus, or residual PGA content (Fig. 1R–1T).

Engineered Cartilage Construction In Vivo

At 2 weeks after implantation, all samples were encapsulated with thick fibrous tissues surrounded by vascular networks (Fig. 2A–2C). Histological examination showed that normal cartilaginous structures with homogeneously distributed lacunas (Fig. 2D, black arrow) and intensely deposited type II collagen (Fig. 2G, black arrow) were observed only in the BMSC group. A smaller number of lacunas and weaker basophilic matrix were seen in the 1:1 group, with similar staining for type II collagen compared with the BMSC group (Fig. 2E, 2H). However, few chondrocytes survived in the AC group, resulting in weak staining of residual type II collagen fibers.

Published Ahead of Print on June 8, 2016 as 10.5966/sctm.2015-0263.

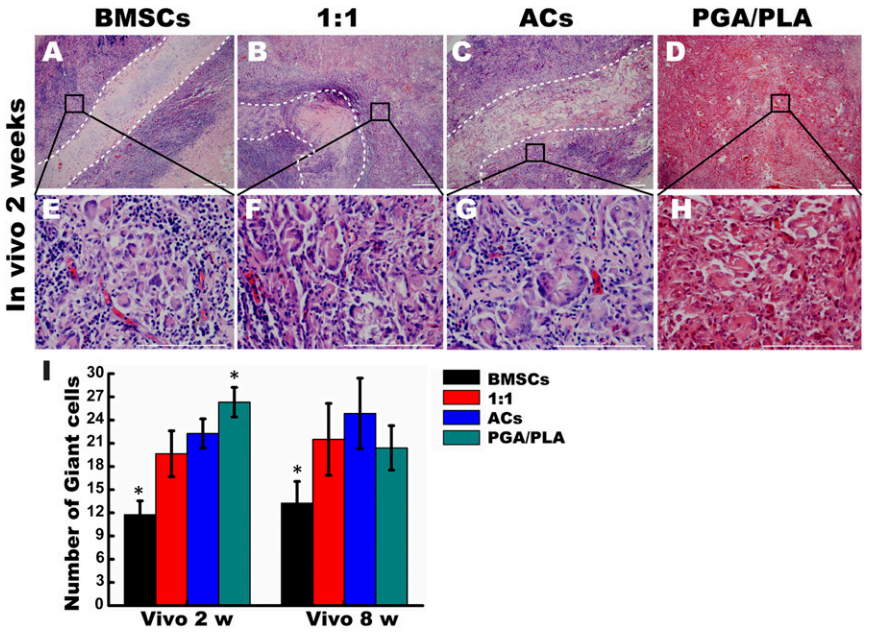

Figure 3. The role of foreign body multinucleated giant cells (FBGCs) in the inflammatory responses to engineered cartilage in vivo. **(A–D):** Representative H&E staining images of engineered cartilage constructs after 2 weeks in vivo at low magnification and the white dotted lines depict the boundary of the implants. **(E–H):** Quantitative comparison of FBGCs from H&E stained images at high magnification after 2 weeks and 8 weeks post implantation among the groups of BMSCs, 1:1, chondrocytes, and PGA/PLA (I). $*$, $p < .05$ (statistically different from other groups). Scale bars = 50 μm **(A–D)** and 100 μm **(E–H)**. Abbreviations: ACs, articular chondrocytes; BMSCs, bone marrow mesenchymal stem cells; PGA, polyglycolic acid; PLA, polylactic acid; w, weeks.

After 8 weeks in vivo, the constructs in the three groups were damaged to varying degrees. Samples in the BMSC group showed several lacunas and positive staining for type II collagen (Fig. 2M, 2P), whereas destructive matrix and a large number of inflammatory cells were observed in the 1:1 (Fig. 2N, 2Q) and AC (Fig. 2O, 2R) groups. Notably, residual PGA fibers were still observed within all groups (Fig. 2M–2O, black arrows).

Analysis of Multinucleated FBGCs

After 2 weeks of implantation, engineered cartilage in the BMSC group maintained a clear boundary with the surrounding fibrous tissue, whereas the cartilaginous matrix was destroyed in the 1:1 and AC groups (Fig. 3A–3C). The encapsulated fibrous tissues in all groups were infiltrated with plenty of multinucleated FBGCs distributed along the implants (Fig. 3E–3H). Furthermore, FBGCs adjacent to the implants ($<$200 μm) were counted, and the results showed that samples in the BMSC group caused the least infiltration of FBGCs compared to the other three groups after 2 and 8 weeks in vivo (Fig. 3I). However, no significant difference was found in the FBGC number between the 1:1 and AC groups. The highest number of FBGCs was seen in the PGA/PLA group after 2 weeks in vivo. These results indicated that BMSC-engineered cartilage had the highest potential for reducing FBGC recruitment.

Analysis of Macrophage and Subsets

To explore the role of macrophages in the inflammatory response to the engineered constructs, the macrophage and the subsets were identified after 72 hours and 2, 4, and 8 weeks in vivo (Fig. 4A–4X; supplemental online Fig. 2). Quantitative analysis showed that the number of cells positive for CD68 (pan-macrophage cell surface marker) was the lowest in the BMSC group at 72 hours and 2 weeks after implantation, indicating that the reduced phagocytosis occurred in the BMSC group. Conversely, in the PGA/PLA group, CD68-positive cells were widespread (Fig. 4D) and significantly more numerous than any other group at 72 hours, 2 and 4 weeks after implantation, which was consistent with the results of multinucleated FBGCs (Fig. 4Y; supplemental online Fig. 2).

Conversely, M2 macrophages indicated by CD206-positive cells maintained the lowest numbers in the PGA/PLA group, but they were significantly higher in the BMSC and 1:1 group compared with the AC group at 2 and 4 weeks in vivo (Fig. 4Z). All these results implied that the BMSC-based engineered cartilage could activate the M2 polarization of macrophages.

Engineered Cartilage Cocultured With Macrophage In Vitro

To further verify the interaction between the engineered cartilage and macrophages, a transwell-based coculture system was established. The experimental model is shown in Figure 5A. After coculturing for 24 hours, the secretion of the proinflammatory factor IL-1β was significantly lower in the BMSC/macrophage (MΦ) coculture group than in the MΦ group (Fig. 5B). In contrast, the anti-inflammatory factor IL-10 was remarkably higher in the BMSC/MΦ and 1:1/MΦ groups than in the MΦ group (Fig. 5C). Moreover, CD68 expression in macrophages stimulated with LPS and IFN-γ showed no differences between all groups, but the fraction of CD206-positive macrophages reached 89.67% $\pm$ 3.71% in the BMSC group and was significantly higher than in the other groups (Fig. 5D, 5M).

Published Ahead of Print on June 8, 2016 as 10.5966/sctm.2015-0263.

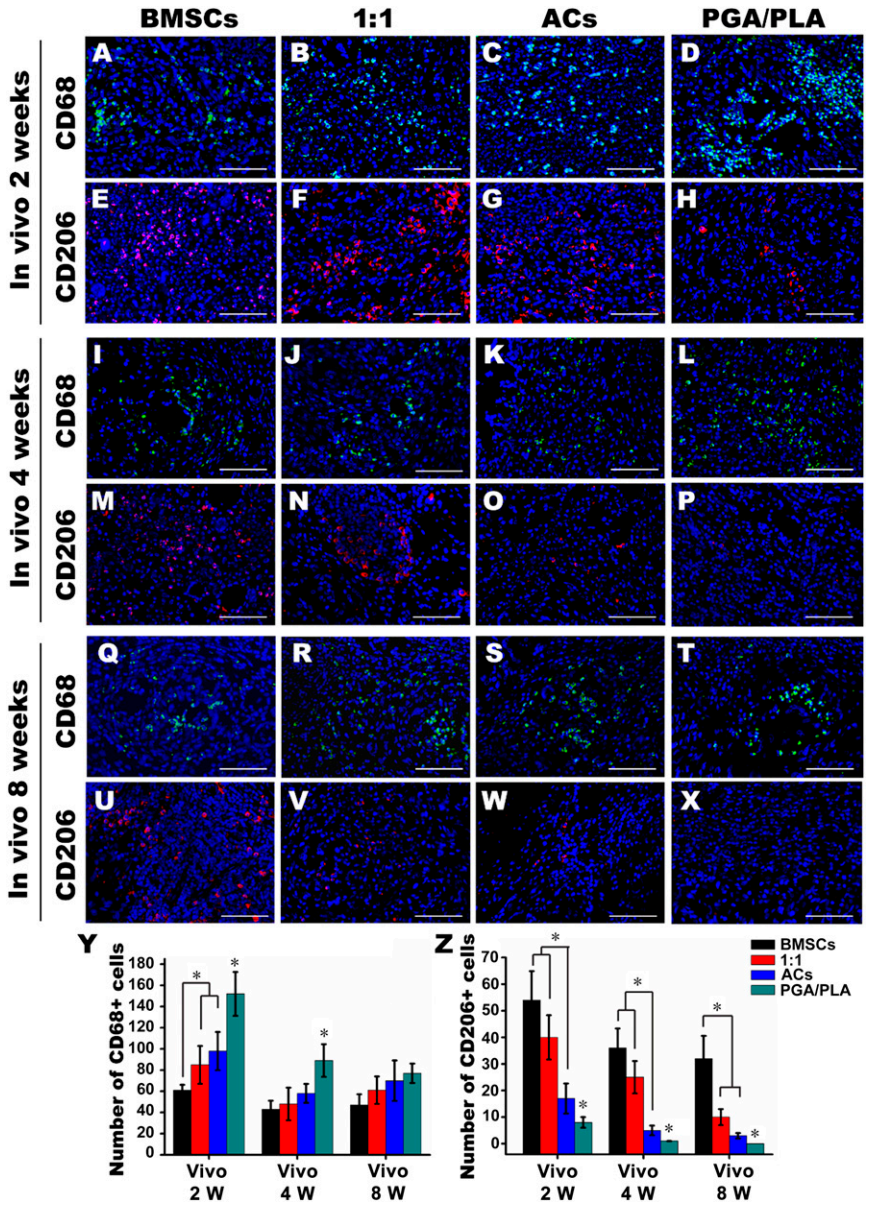

Figure 4. The role of macrophages in the inflammatory response to the engineered cartilage in vivo. Immunofluorescent staining of CD68 (green) and CD206 (red) colocalized with 4′,6-diamidino-2-phenylindole-stained nuclei (blue) after 2 **(A–H)**, 4 **(I–P)**, and 8 **(Q–X)** weeks after implantation. **(Y, Z):** Quantitative comparison of CD68- and CD206-positive cells among the groups of BMSCs, 1:1, chondrocytes, and PGA/PLA. Scale bars = 50 μm. $*$, $p < .05$ (statistically different from other groups). Abbreviations: ACs, articular chondrocytes; BMSCs, bone marrow mesenchymal stem cells; PGA, polyglycolic acid; PLA, polylactic acid; W, weeks.

Differential Expressions of Polarization-Related Genes in Macrophages After Coculturing With Engineered Cartilage

To confirm M2 polarization of macrophages under this coculture system, the expressions of different inflammatory factors and chemokines receptors indicative of M1 and M2 polarization were examined. The results showed that the mRNA expression of proinflammatory cytokines, including IL-1β, TNF-α, IL-6, and inducible nitric oxide synthase 2 (iNOS II), were significantly downregulated in the BMSC/MΦ coculture group compared with the MΦ group, whereas similar expression levels were found in the 1:1/MΦ and AC/MΦ groups (Fig. 6A–6D). In contrast, the anti-inflammatory cytokines IL-10 and TGF-β were significantly higher in the BMSC/MΦ coculture group compared with the other groups, and the BMSC/MΦ coculture group also had a higher expression of arginase 1 (Arg-1) than in the MΦ group (Fig. 6E–6G). Moreover, positive markers of M1 macrophage, including chemokine (C-C motif) receptor type 1 (CCR1), chemokine (C-C motif) receptor type 4 (CCR4), chemokine (C-X-C motif) receptor type 2 (CXCR2), and chemokine (C-X3-C motif) receptor type 1 (CX3CR1), showed the lowest expression levels in the BMSC/MΦ coculture group, but the highest in the AC/MΦ group (Fig. 6I–6L). Additionally, the mRNA level of CCR2 was significantly higher in the BMSC/MΦ coculture group than in the other three groups (Fig. 6H).

Published Ahead of Print on June 8, 2016 as 10.5966/sctm.2015-0263.

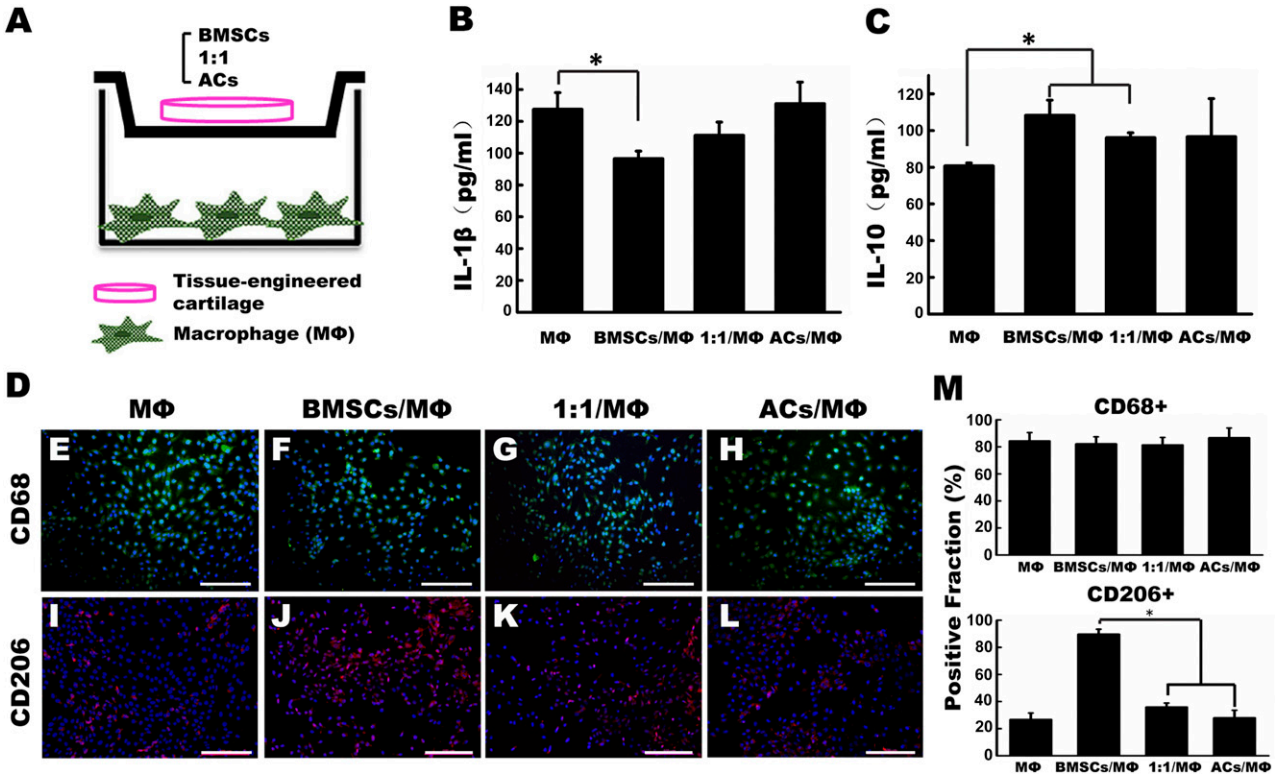

Figure 5. In vitro coculture of engineered cartilage and activated macrophage for 24 hours. **(A):** Coculturing of different groups of engineered cartilage with macrophages in a transwell system. **(B, C):** Comparison of the protein concentrations of the proinflammatory factor IL-1β **(B)** and anti-inflammatory factor IL-10 **(C)** secreted by macrophages in the supernatant among different coculture groups. **(E–M):** After coculturing with different engineered cartilage for 24 hours, macrophages were immunofluorescent stained of CD68 (green) **(E–H)** and CD206 (red) **(I–L)**, and their positive fractions were calculated **(M)**. Scale bars = 50 μm. $*$, $p < .05$ (statistically different from other groups). Abbreviations: ACs, articular chondrocytes; BMSCs, bone marrow mesenchymal stem cells; IL-1β, interleukin 1β; IL-10, interleukin 10; MΦ, macrophages.

Discussion

There have been very few reports on the successful construction of tissue-engineered cartilage in immunocompetent animal models, although tissue-engineered cartilage could be generally accomplished in nude mice. The inflammatory response to the scaffold has been regarded as the main reason for the destruction and resorption of autologous engineered cartilage. To find a strategy for promoting the survival of engineered cartilage, here we took advantage of the immunomodulatory capacity of BMSCs to ameliorate the inflammation induced by the scaffold in a pig model. As to the immunosuppressive characteristic of BMSCs, conflicting results have been produced in chondrogenically differentiated cells. Ryan et al. showed that the chondrogenic differentiation of MSCs could increase the host antidonor immune responses after its allogenic transplantation [27]. Another study that highlighted both of the MSCs and MSC-differentiated chondrocytes found that they showed similar properties in suppressing T-cell responses in an allogenic model [28]. Most of these studies investigated the immunological consequences of BMSC chondrogenic differentiation in an allogeneic model, with less attention to the inflammation responses in an autograft model. In our study, autogenic BMSCs were seeded on a PGA/PLA scaffold and cultured in chondrogenic differentiation medium, and we focused on the inflammation induced by the PGA/PLA scaffold in vivo and the interaction between the macrophage and the whole cell-scaffold complex. We demonstrated that BMSC-engineered cartilage showed the less inflammatory phenotype by increasing M2 polarization of macrophages, resulting in better tissue survival at 8 weeks after implantation compared with those regenerated by chondrocytes alone or in combination with BMSCs.

Several studies have reported that the inflammatory response caused by tissue-engineered implants showed a strong association with the used scaffolds and/or their degradation products [3, 4, 6]. PGA, which has been used in sutures and wound dressings since the 1970s, was found to have good biocompatibility for cartilage tissue engineering [8]. PLA, which is also U.S. Food and Drug Administration-approved, was usually used to coat PGA fibers to maintain a fixed porous structure and increase the stiffness. We chose PGA/PLA to construct tissue-engineered cartilage because of its superiority in the balance of degradability and shape control, which are very important for the regeneration of auricular or nasal cartilage that requires a high fidelity of configuration fit to the defect shape. However, residual PGA/PLA and its degradation products can cause a decrease in local pH, resulting in inflammation, even though the degradation products are harmless [8]. This inflammatory process is accompanied by the recruitment of macrophages and the accumulation of FBGCs, which are believed to induce oxidative damage and cause chronic inflammation [29]. In our study, all three groups of complexes formed cartilage-like tissues in vitro; however, after 8 weeks

Published Ahead of Print on June 8, 2016 as 10.5966/sctm.2015-0263.

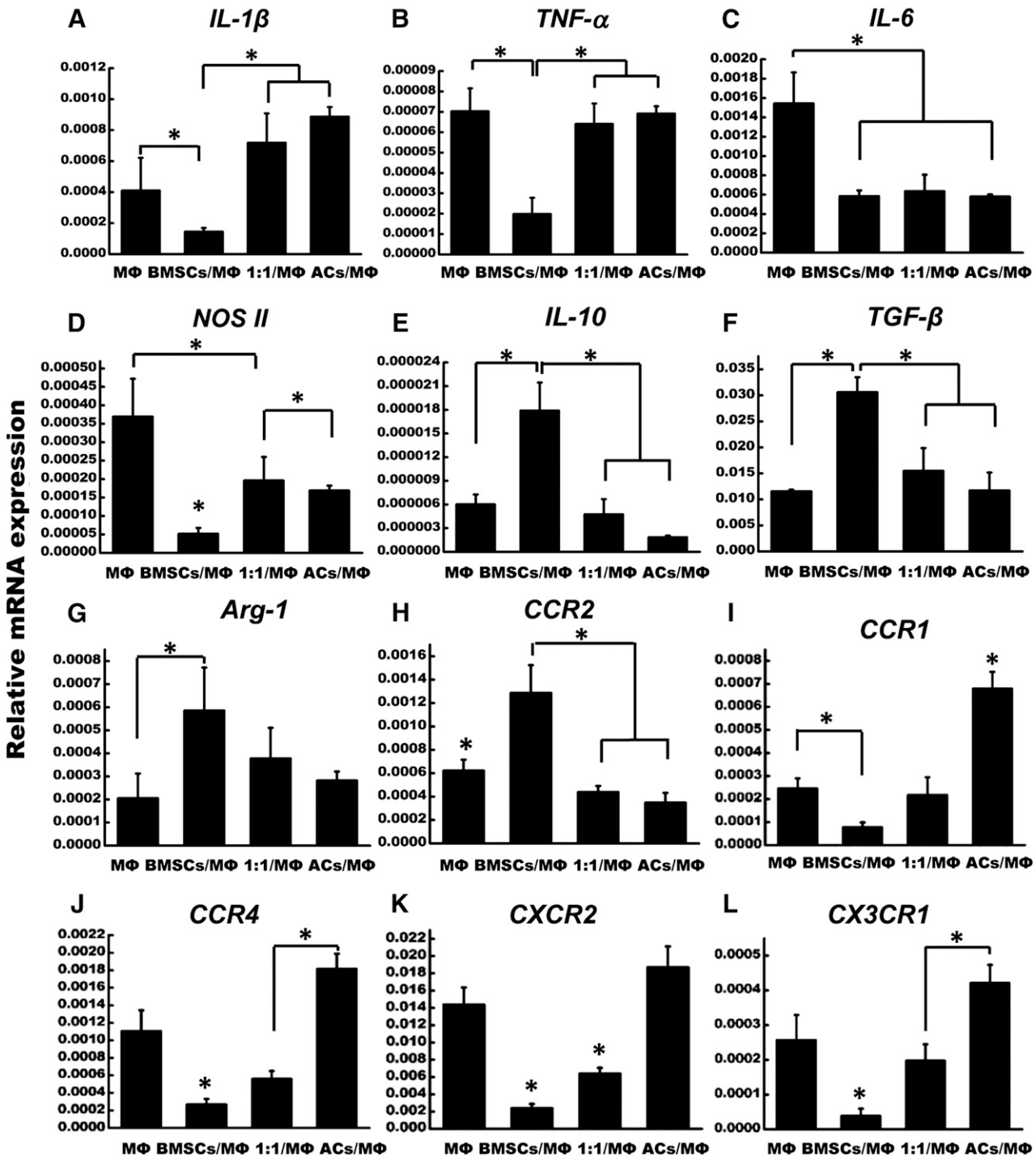

Figure 6. Quantitative analysis of inflammation and chemokine receptors related genes in macrophages after coculturing with different groups of engineered cartilage for 24 hours. ∗, $p < .05$ (statistically different from other groups). Abbreviations: ACs, articular chondrocytes; *Arg-1*, arginase 1; BMSCs, bone marrow mesenchymal stem cells; *CCR1*, chemokine (C-C motif) receptor type 1; *CCR2*, chemokine (C-C motif) receptor type 2; *CCR4*, chemokine (C-C motif) receptor type 4; *CXCR2*, chemokine (C-X-C motif) receptor type 2; *CX3CR1*, chemokine (C-X3-C motif) receptor type 1; *IL-1β*, interleukin 1β; *IL-6*, interleukin 6; *IL-10*, interleukin 10; MΦ, macrophages; *NOS II*, nitric oxide synthase 2; *TGF-β*, transforming growth factor β; *TNF-α*, tumor necrosis factor α.

in vivo, the constructs in the AC and 1:1 groups were all damaged, whereas those in the BMSC group maintained partial cartilaginous structure with the fewest FBGCs and CD68-positive macrophages. The engineered cartilage in the 1:1 group also showed a limited effect on M2 polarization of macrophage at the early stage of 2 and 4 weeks after implantation. It implied that increasing the ratio of BMSCs:ACs in the coculture group might improve the quality of engineered cartilage and maintain tissue homeostasis in the subcutaneous environment of a pig model. However, the main potential pitfall

Published Ahead of Print on June 8, 2016 as 10.5966/sctm.2015-0263.

associated with using BMSCs as seed cells for cartilage engineering is the induction of hypertrophy and calcification [25]. In the present study, BMSC-engineered cartilage was superior in inflammation resistance compared with other groups, and the hypertrophy of BMSC-engineered cartilage was not very obvious in the FBS-free-medium culture condition.

Reports have shown that inflammatory reactions against tissue-engineered implants were mediated mainly by macrophages, which played an indispensable role in tissue homeostasis and defense. Macrophages can be phenotypically polarized by the microenvironment in two main forms: the classically activated macrophages (or M1) that display a proinflammatory profile, and the alternatively activated macrophages (or M2) that exhibit an anti-inflammatory property [30–32]. The capability of macrophages to express distinct functional phenotypes is typically manifested in pathological conditions, including various infectious and inflammatory diseases [33]. M2 macrophages appear to be one of the major players in the resolution of inflammation through high endocytic clearance capacities, trophic factor synthesis, and anti-inflammatory cytokine secretion [34]. A previous report revealed that activated macrophages cocultured with MSCs expressed high levels of CD206, IL-10, and IL-6, but low levels of IL-12 and TNF-α, which were identified as a novel subtype of M2 macrophage with a potentially significant role in tissue repair [30]. Our data demonstrated that BMSC-based engineered cartilage could accelerate M2 polarization of macrophages in vivo, and stimulated macrophages cocultured with BMSC-engineered cartilage expressed the highest levels of CD206 and anti-inflammatory factors IL-10 and TGF-β and the lowest levels of the proinflammatory factors TNF-α, IL-6, IL-1β, and iNOS II. Additionally, Arg-1, an enzyme used by M2 macrophages to convert arginine into ornithine, was remarkably elevated in the BMSC/MΦ group, implying a shift from M1 to M2 phenotype macrophages [24, 33, 35]. It was reported that a predominant activation of nuclear factor κB and signal transducer and activator of transcription 1 (STAT1) promoted M1 macrophage polarization, whereas STAT3 and STAT6 participated in the promotion of M2 polarization [36, 37]. The underlying mechanism of BMSC-engineered cartilage inducing the M2 macrophage phenotype should be investigated in the future.

Chemokines are a structurally related family of cytokines that are classified into four subpopulations—CC, CXC, CX3C, and XC—which are believed to be major mediators in macrophage recruitment. Shechter et al. showed that M1 and M2 macrophages were sequentially recruited to the injury site from different sources by distinct chemokines [38]. Similarly, Xuan et al. suggested that chemokines differentially enabled the chemotaxis of macrophages of different subtypes by modulating chemokine receptor expression and their corresponding signal transduction [39]. For example, CCL19, CCL21, CCL24, CCL25, CXCL8, CXCL10, and CXCL2 specifically induce M1 macrophage chemotaxis [38], whereas CCL2, CCL5, CXCL10, and CXCL12 promote M2 macrophage migration [40]. Our data showed a remarkably increased expression of CCR2 in macrophages cocultured with BMSC-engineered cartilage after 24 hours, which was in accordance with the results of Sierra-Filardi et al. and Sun et al. [41, 42], who demonstrated that the CCL2-CCR2 axis promoted M2 macrophage polarization by influencing the expression of functionally relevant and polarization-associated genes and down-modulating proinflammatory cytokine production. In addition, we also found that macrophages cocultured with BMSC-engineered cartilage exhibited a significant decrease in the mRNA expression of CCR1, CCR4, CXCR2, and CX3CR1, which were reported to be extensively distributed on the surface of M1 macrophages [39]. However, the specific roles of chemokines in macrophage polarization remain controversial, and the chemotactic signals released by the engineered cartilage might not necessarily correlate with the expression of different chemokines. There were also other groups that have shown that M2 macrophages were recruited through sphingosine-1-phosphate receptors [43]. Further screening is required to determine the mechanism of macrophage recruitment and polarization.

Conclusion

Overcoming the inflammation induced by the implants is a challenge for the survival and clinical application of tissue-engineered cartilage. In the present study, we demonstrated that BMSC-based engineered cartilage could suppress in vivo inflammation by increasing M2 polarization of macrophages, resulting in better tissue survival 8 weeks after subcutaneous implantation in pigs compared with those regenerated by chondrocytes alone or in combination with BMSCs. This was further supported by the in vitro coculture findings, including the increased releasing of IL-10 and the decreased secretion of IL-1β in the supernatant, and the upregulation of CD206 and the gene expression changes in alignment with the M1-to-M2 transition in macrophages cocultured with BMSC-engineered cartilage. Therefore, using BMSCs as seed cells for cartilage engineering has good potential to suppress the inflammation induced by the PGA/PLA scaffold and improve the tissue survival in immunocompetent environment.

Acknowledgments

This work was supported by Beijing Municipal Science and Technology Project D090800046609003; National Natural Science Foundation of China Grants 31300801, 81471804, and 31300807; and Beijing Natural Science Foundation Grant 7144239.

Author Contributions

J.D.: collection and/or assembly of data, data analysis and interpretation, manuscript writing; B.C.: financial support, collection and/or assembly of data; T.L., X.L., X.F., Q.W., and L.Y.: provision of study materials, collection and/or assembly of data; N.K., Y.C., and R.X.: conception and design, financial support, data analysis and interpretation, final approval of manuscript.

Disclosure of Potential Conflicts of Interest

The authors indicated no potential conflicts of interest.

References

1 Funayama A, Niki Y, Matsumoto H et al. Repair of full-thickness articular cartilage defects using injectable type II collagen gel embedded with cultured chondrocytes in a rabbit model. J Orthop Sci 2008;13:225–232.

2 Xie J, Han Z, Naito M et al. Articular cartilage tissue engineering based on a mechano-active scaffold made of poly (L-lactide-co-epsilon-caprolactone): In vivo performance in adult rabbits. J Biomed Mater Res B Appl Biomater 2010;94:80–88.

3 Kanazawa S, Fujihara Y, Sakamoto T et al. Tissue responses against tissue-engineered

Published Ahead of Print on June 8, 2016 as 10.5966/sctm.2015-0263.

cartilage consisting of chondrocytes encapsulated within non-absorbable hydrogel. J Tissue Eng Regen Med 2013;7:1–9.

4 Asawa Y, Sakamoto T, Komura M et al. Early stage foreign body reaction against biodegradable polymer scaffolds affects tissue regeneration during the autologous transplantation of tissue-engineered cartilage in the canine model. Cell Transplant 2012;21: 1431–1442.

5 Shieh SJ, Terada S, Vacanti JP. Tissue engineering auricular reconstruction: In vitro and in vivo studies. Biomaterials 2004;25:1545–1557.

6 Vallés G, Bensiamar F, Crespo L et al. Topographical cues regulate the crosstalk between MSCs and macrophages. Biomaterials 2015; 37:124–133.

7 Bichara DA, Pomerantseva I, Zhao X et al. Successful creation of tissue-engineered autologous auricular cartilage in an immunocompetent large animal model. Tissue Eng Part A 2014;20: 303–312.

8 Boland ED, Telemeco TA, Simpson DG et al. Utilizing acid pretreatment and electrospinning to improve biocompatibility of poly (glycolic acid) for tissue engineering. J Biomed Mater Res B Appl Biomater 2004;71:144–152.

9 Liu Y, Zhang L, Zhou G et al. In vitro engineering of human ear-shaped cartilage assisted with CAD/CAM technology. Biomaterials 2010; 31:2176–2183.

10 Fujihara Y, Takato T, Hoshi K. Macrophage-inducing FasL on chondrocytes forms immune privilege in cartilage tissue engineering, enhancing in vivo regeneration. STEM CELLS 2014;32: 1208–1219.

11 Zheng L, Sun J, Chen X et al. In vivo cartilage engineering with collagen hydrogel and allogenous chondrocytes after diffusion chamber implantation in immunocompetent host. Tissue Eng Part A 2009;15:2145–2153.

12 Xu J, Li L, Xiong J et al. Cyclophosphamide combined with bone marrow mesenchymal stromal cells protects against bleomycin-induced lung fibrosis in mice. Ann Clin Lab Sci 2015;45:292–300.

13 Lan YW, Choo KB, Chen CM et al. Hypoxia-preconditioned mesenchymal stem cells attenuate bleomycin-induced pulmonary fibrosis. Stem Cell Res Ther 2015;6:97.

14 Shen Q, Chen B, Xiao Z et al. Paracrine factors from mesenchymal stem cells attenuate epithelial injury and lung fibrosis. Mol Med Rep 2015;11:2831–2837.

15 Németh K, Leelahavanichkul A, Yuen PS et al. Bone marrow stromal cells attenuate sepsis via prostaglandin E(2)-dependent reprogramming of host macrophages to increase their interleukin-10 production. Nat Med 2009;15: 42–49.

16 Ho MS, Mei SH, Stewart DJ. The immunomodulatory and therapeutic effects of mesenchymal stromal cells for acute lung injury and sepsis. J Cell Physiol 2015;230:2606–2617.

17 Walter J, Ware LB, Matthay MA. Mesenchymal stem cells: Mechanisms of potential therapeutic benefit in ARDS and sepsis. Lancet Respir Med 2014;2:1016–1026.

18 Choi H, Lee RH, Bazhanov N et al. Anti-inflammatory protein TSG-6 secreted by activated MSCs attenuates zymosan-induced mouse peritonitis by decreasing TLR2/NF-κB signaling in resident macrophages. Blood 2011;118:330–338.

19 Buda R, Vannini F, Cavallo M et al. Osteochondral lesions of the knee: A new one-step repair technique with bone-marrow-derived cells. J Bone Joint Surg Am 2010;92(suppl 2):2–11.

20 Wakitani S, Nawata M, Tensho K et al. Repair of articular cartilage defects in the patellofemoral joint with autologous bone marrow mesenchymal cell transplantation: Three case reports involving nine defects in five knees. J Tissue Eng Regen Med 2007;1:74–79.

21 Enea D, Cecconi S, Calcagno S et al. Single-stage cartilage repair in the knee with microfracture covered with a resorbable polymer-based matrix and autologous bone marrow concentrate. Knee 2013;20:562–569.

22 Bornes TD, Jomha NM, Mulet-Sierra A et al. Hypoxic culture of bone marrow-derived mesenchymal stromal stem cells differentially enhances in vitro chondrogenesis within cell-seeded collagen and hyaluronic acid porous scaffolds. Stem Cell Res Ther 2015;6:84.

23 Swartzlander MD, Blakney AK, Amer LD et al. Immunomodulation by mesenchymal stem cells combats the foreign body response to cell-laden synthetic hydrogels. Biomaterials 2015;41:79–88.

24 Geng Y, Zhang L, Fu B et al. Mesenchymal stem cells ameliorate rhabdomyolysis-induced acute kidney injury via the activation of M2 macrophages. Stem Cell Res Ther 2014;5:80.

25 Kang N, Liu X, Guan Y et al. Effects of co-culturing BMSCs and auricular chondrocytes on the elastic modulus and hypertrophy of tissue engineered cartilage. Biomaterials 2012;33: 4535–4544.

26 Yan D, Zhou G, Zhou X et al. The impact of low levels of collagen IX and pyridinoline on the mechanical properties of in vitro engineered cartilage. Biomaterials 2009;30:814–821.

27 Ryan AE, Lohan P, O'Flynn L et al. Chondrogenic differentiation increases antidonor immune response to allogeneic mesenchymal stem cell transplantation. Mol Ther 2014;22: 655–667.

28 Zheng ZH, Li XY, Ding J et al. Allogeneic mesenchymal stem cell and mesenchymal stem cell-differentiated chondrocyte suppress the responses of type II collagen-reactive T cells in rheumatoid arthritis. Rheumatology (Oxford) 2008;47:22–30.

29 McNally AK, Anderson JM. Foreign body-type multinucleated giant cell formation is potently induced by alpha-tocopherol and prevented by the diacylglycerol kinase inhibitor R59022. Am J Pathol 2003;163:1147–1156.

30 Kim J, Hematti P. Mesenchymal stem cell-educated macrophages: A novel type of alternatively activated macrophages. Exp Hematol 2009;37:1445–1453.

31 Mantovani A, Biswas SK, Galdiero MR et al. Macrophage plasticity and polarization in tissue repair and remodelling. J Pathol 2013;229:176–185.

32 Wolf MT, Dearth CL, Ranallo CA et al. Macrophage polarization in response to ECM coated polypropylene mesh. Biomaterials 2014;35:6838–6849.

33 Mosser DM, Edwards JP. Exploring the full spectrum of macrophage activation. Nat Rev Immunol 2008;8:958–969.

34 Martinez FO, Sica A, Mantovani A et al. Macrophage activation and polarization. Front Biosci 2008;13:453–461.

35 Brown BN, Valentin JE, Stewart-Akers AM et al. Macrophage phenotype and remodeling outcomes in response to biologic scaffolds with and without a cellular component. Biomaterials 2009;30:1482–1491.

36 Sica A, Mantovani A. Macrophage plasticity and polarization: In vivo veritas. J Clin Invest 2012;122:787–795.

37 Gao S, Mao F, Zhang B et al. Mouse bone marrow-derived mesenchymal stem cells induce macrophage M2 polarization through the nuclear factor-κB and signal transducer and activator of transcription 3 pathways. Exp Biol Med (Maywood) 2014;239:366–375.

38 Shechter R, Miller O, Yovel G et al. Recruitment of beneficial M2 macrophages to injured spinal cord is orchestrated by remote brain choroid plexus. Immunity 2013;38: 555–569.

39 Xuan W, Qu Q, Zheng B et al. The chemotaxis of M1 and M2 macrophages is regulated by different chemokines. J Leukoc Biol 2015;97: 61–69.

40 Vogel DY, Heijnen PD, Breur M et al. Macrophages migrate in an activation-dependent manner to chemokines involved in neuroinflammation. J Neuroinflammation 2014;11:23.

41 Sierra-Filardi E, Nieto C, Domínguez-Soto A et al. CCL2 shapes macrophage polarization by GM-CSF and M-CSF: Identification of CCL2/CCR2-dependent gene expression profile. J Immunol 2014;192:3858–3867.

42 Sun L, Louie MC, Vannella KM et al. New concepts of IL-10-induced lung fibrosis: Fibrocyte recruitment and M2 activation in a CCL2/CCR2 axis. Am J Physiol Lung Cell Mol Physiol 2011;300:L341–L353.

43 Das A, Segar CE, Hughley BB et al. The promotion of mandibular defect healing by the targeting of S1P receptors and the recruitment of alternatively activated macrophages. Biomaterials 2013;34:9853–9862.

See www.StemCellsTM.com for supporting information available online.

